ARTICLE

Co-delivery of Cisplatin and Rapamycin for Enhanced Anticancer Therapy through Synergistic Effects and Microenvironment Modulation

Shutao Guo,* C. Michael Lin, Zhenghong Xu, Lei Miao, Yuhua Wang, and Leaf Huang*

Division of Molecular Pharmaceutics and Center for Nanotechnology in Drug Delivery, Eshelman School of Pharmacy, University of North Carolina at Chapel Hill, Chapel Hill, North Carolina 27599, United States

ABSTRACT The tumor microenvironment plays an important role in the tumor's progression and metastasis. Therefore, successful alteration of this delicate setting against the tumor's favor can open a window for therapeutic efficacy. We have developed a modality to bring about treatment-induced alterations in the tumor microenvironment by employing the synergistic effects between two drugs. Co-delivery of rapamycin (RAPA), an mTOR inhibitor that may offer notable therapy through antiangiogenic activity, alongside cisplatin can foster significant potency as RAPA sensitizes A375 melanoma cells to cisplatin therapy through microenvironment modulation. However, encapsulation of these drugs into poly(lactic-*co*-glycolic acid) (PLGA) NPs was inefficient due to the incompatibility between the two free drugs and the polymer matrix. Here, we show cisplatin can be made hydrophobic by coating a nanoprecipitate (cores) of the drug with dioleoylphosphatidic acid (DOPA). These DOPA coated cisplatin cores are compatible with PLGA and can be coencapsulated in PLGA NPs alongside RAPA at a molar ratio to promote synergistic antitumor activity. The presence of the cisplatin cores significantly improved the encapsulation of RAPA into PLGA NPs. Furthermore, PLGA NPs containing both cisplatin cores and RAPA induced significant apoptosis on A375-luc human melanoma cells *in vitro*. Additionally, they inhibited the growth of A375-luc melanoma in a xenograft tumor model through modulation of the tumor vasculature and permitted enhanced penetration of NPs into the tumor.

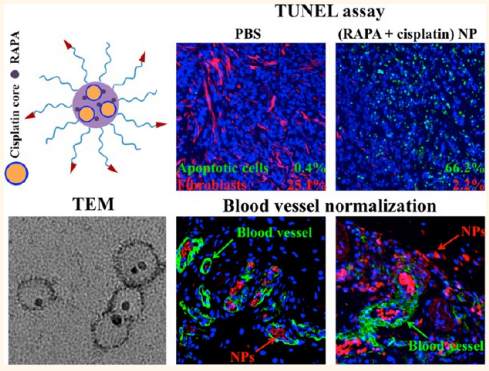

KEYWORDS: Tumor microenvironment · synergistic effect · antiangiogenesis · cisplatin · rapamycin · combination therapy · PLGA

The advancement of nanomedicine is currently focused on amplifying the *in vivo* stability and pharmacokinetics of formulations in an effort to enhance drug delivery.[1] However, tumor-specific abnormalities in the microenvironment such as high interstitial fluid pressure (IFP) play a critical role in hindering treatment efficacy and can result in undesirably low drug penetration while contributing to drug resistance.[2] Specifically, tumor-associated fibroblasts (TAFs), a primary component of the tumor microenvironment, play a key role in defining the role and extent of tumor proliferation.[3] Therefore, successfully remodeling the tumor microenvironment against the conditions necessary for proliferation may be a powerful strategy to sensitize tumor cells to chemotherapy.[4−8]

The application of combination therapy can be achieved through coadministration of an additional drug alongside the sensitizer.[9−12] The interaction between two drugs is dependent on the dose ratio between the drugs and can be synergistic or potentially antagonistic.[13,14] Therefore, the importance of maintaining the synergistic therapeutic ratio throughout the nanoparticle (NP) formulation cannot be overlooked. The process of coencapsulating two drugs into a single NP proves difficult if the drugs differ greatly in their physicochemical properties. Therefore, formulations, which are capable of encapsulating and delivering multiple drugs with diverse physicochemical properties while maintaining the controlled synergistic ratio, are thus desired.

* Address correspondence to guost@email.unc.edu, leafh@unc.edu.

Received for review February 23, 2014 and accepted April 10, 2014.

Published online April 10, 2014
10.1021/nn5010815

Scheme 1. Efficient co-encapsulation of cisplatin cores and RAPA into PLGA NP using a solvent displacement technique[a]

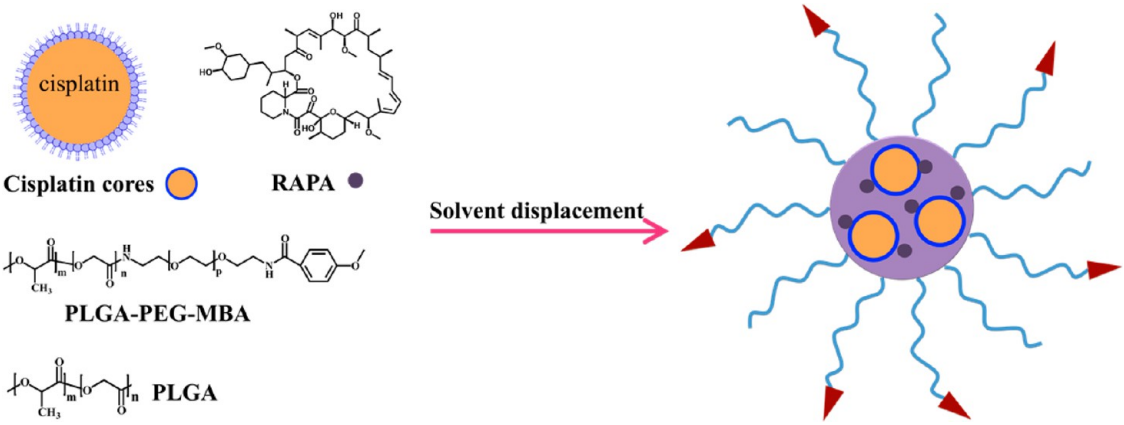

[a] *p*-Methoxybenzylamide (MBA), i.e. anisamide, was added as a targeting ligand.

Rapamycin (RAPA), an mTOR inhibitor, inhibits primary and metastatic tumor growth by antiangiogenesis through decreasing the production of vascular endothelial growth factor (VEGF) and lowering the response of vascular endothelial cells to stimulation by VEGF.[15,16] Recent studies have shown that RAPA also mediates vascular renormalization, resulting in improved tumor perfusion.[17] While RAPA cannot be effectively administered via intravenous (IV) injection, its hydrophobicity can be employed to facilitate the encapsulation of RAPA into PLGA NPs. While this has been achieved previously, a high drug loading was difficult to attain due to incompatibility between the drug and polymer matrix.[18] It is known that RAPA can sensitize cells to cisplatin through the down regulation of antiapoptotic proteins such as p53-induced p21.[19−21] As a result, combination therapy with both cisplatin and RAPA can utilize the synergy between both drugs for enhanced anticancer efficacy. Yet, current efforts at encapsulating cisplatin into PLGA NPs through the double emulsion method are severely hampered by a low drug loading and the presence of burst drug release.[1]

Previously, we have developed lipid-coated calcium phosphate cores with a surface layer coating of dioleoylphosphatidic acid (DOPA). The hydrophobic cores are capable of efficiently encapsulating gemcitabine triphosphate,[22] small interfering RNA (siRNA),[23] DNA,[24] peptides,[25] and other types of hydrophilic phosphorylated drugs. In an effort to exploit this method for cisplatin encapsulation, a formulation was developed where cisplatin composes both the drug and the nanocarrier itself. These DOPA-coated cisplatin cores,[25,26] which are composed entirely of cisplatin, are characterized by a substantial drug loading and share similar surface properties with oleic acid coated iron oxide NPs (IONP) and quantum dots (QD).[27−30] Since IONPs and QDs have been efficiently loaded into PLGA NPs and enhanced the encapsulation of hydrophobic drugs alongside them, we hoped to coencapsulate our cisplatin cores, along with RAPA into PLGA NPs using the solvent displacement method. Sigma receptors are well-known membrane-bound proteins that show high affinity for neuroleptics and are overexpressed on many human tumors including melanoma.[31−33] Therefore, anisamide, an agonist of sigma receptors, was conjugated to PLGA−PEG to enhance the delivery of drugs into A375-luc human melanoma cells.

Herein, we report an efficient coencapsulation of both cisplatin cores and RAPA into micelle-like PLGA-PEG-anisamide (MBA) NPs using the solvent displacement method (Scheme 1). Anticancer efficacy of this formulation was investigated both *in vitro* and *in vivo*. We hypothesized that codelivery of both drugs would result in enhanced anticancer efficacy by modulating the tumor microenvironment to improve the penetration of PLGA NPs into the tumor. The study was performed in a xenograft model of human melanoma.

RESULTS AND DISCUSSION

Encapsulation of Cisplatin Cores and RAPA into PLGA NPs Using Solvent Displacement Method. Cisplatin is a first-line therapy against a wide spectrum of solid neoplasms. However, systemic toxicities including nephro- and neurotoxicities along with drug resistance severely limit the use of cisplatin in the clinical setting.[34−36] In an effort to overcome the associated nephro- and neurotoxicities, attempts to encapsulate cisplatin into NPs were made. However, these attempts were hampered by the poor solubility of cisplatin in water and oil. By exploiting this previous barrier to our advantage, we have succeeded in the synthesis of cisplatin cores with substantial drug loading through a reverse microemulsion method.[26] The resulting cisplatin cores are composed entirely of cisplatin and stabilized by DOPA with a drug loading of approximately 93 wt % and have tunable sizes between 12 and 75 nm.[25,26] After being coated with an outer leaflet lipid layer, cisplatin cores

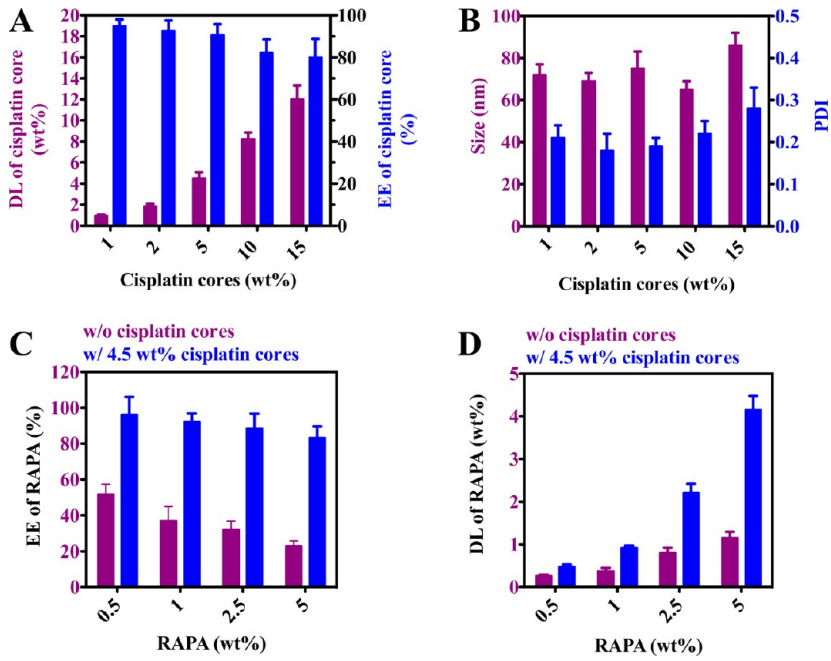

Figure 1. DL and EE of cisplatin PLGA NPs (A); size and PDI (polydispersity index) of cisplatin PLGA NPs (B); EE of RAPA in PLGA NPs in the absence or presence of 4.5 wt % cisplatin cores (C); DL of RAPA in PLGA NPs in the absence or presence of cisplatin cores (D). Key: DL, drug loading; EE, encapsulation efficiency. Size and PDI were measured by DLS.

demonstrated potent antitumor effects both *in vivo* and *in vitro*.

It is notable that the hydrophobic surface coating of cisplatin cores permits their solubility in organic solvents including hexane, chloroform, and tetrahydrofuran (THF).[26] Here, we attempted to encapsulate cisplatin cores inside PLGA NPs (cisplatin PLGA NPs) using the solvent displacement method (Scheme 1). THF is a water-miscible, volatile solvent and is versatile for dissolving a variety of hydrophobic compounds. Thus, THF was selected as the solvent along with water as the antisolvent for solvent displacement process. When the PLGA-PEG-MBA polymer was self-assembled into NPs, hydrophobic cisplatin cores (~12 nm) were efficiently encapsulated into PLGA NPs through hydrophobic interaction. The drug loading (DL) of cisplatin cores was determined using inductively coupled plasma mass spectrometry (ICP-MS) (Figure 1A). When the feed ratio of cisplatin cores was lower than 5.0 wt %, the encapsulation efficiency (EE) was higher than 90%. Notably, over 82% of cisplatin cores were encapsulated and a 12 wt % DL was achieved when the feed ratio of cisplatin cores was at 15 wt %. This is the first time that cisplatin has been encapsulated into PLGA NPs using solvent displacement, and its DL is much higher than other current cisplatin PLGA formulations. In addition, DLS results showed cisplatin PLGA NPs were approximately 80 nm in size and exhibited a monodisperse distribution (Figure 1B).

Our success in efficiently loading cisplatin cores into PLGA NPs offers a new opportunity to codeliver two drugs for combination therapy. For example, hydrophobic cisplatin cores can be engineered into PLGA NPs with other hydrophobic anticancer drugs simultaneously, such as paclitaxel and RAPA. Here, RAPA was further chosen and encapsulated into PLGA NPs alongside cisplatin cores, due to its synergy with cisplatin. The loading of RAPA was measured using HPLC. The first attempts at loading RAPA alone within PLGA NPs (RAPA PLGA NPs) at a feed ratio of 5.0 wt % resulted in a low EE of only 23%, correlating to a DL of 1.15 wt % (Figure 1C). It is because RAPA is encapsulated into the polymer matrix of PLGA NPs through hydrophobic interactions. Therefore, the encapsulation is limited by the compatibility between RAPA and the hydrophobic block copolymer.[37−39] However, when RAPA was coencapsulated alongside 4.5 wt % cisplatin cores at a 5.0 wt % feed ratio (combinatory PLGA NPs), the EE and DL of RAPA in combinatory PLGA NPs were subsequently increased to 80% and 4.0 wt % (Figure 1D), respectively. Therefore, we noticed that the presence of cisplatin cores significantly enhanced the DL of RAPA by 3.5-fold. Even when the feed ratio of RAPA was decreased to 2.5 wt % alongside 4.5 wt % of cisplatin cores, the DL of RAPA in combinatory PLGA NPs was 2.2 wt % and the EE of RAPA was still facilitated by 2.8-fold in the presence of the cisplatin cores. This finding is consistent with previous observations that oleic acid coated NPs can enhance encapsulation of hydrophobic drugs in PLGA NP.[40−42] DLS results confirmed that the size and monodispersity of all PLGA NPs was not affected by the encapsulation of RAPA, cisplatin cores, or both drugs in a single NP (Figure S1, Supporting Information).

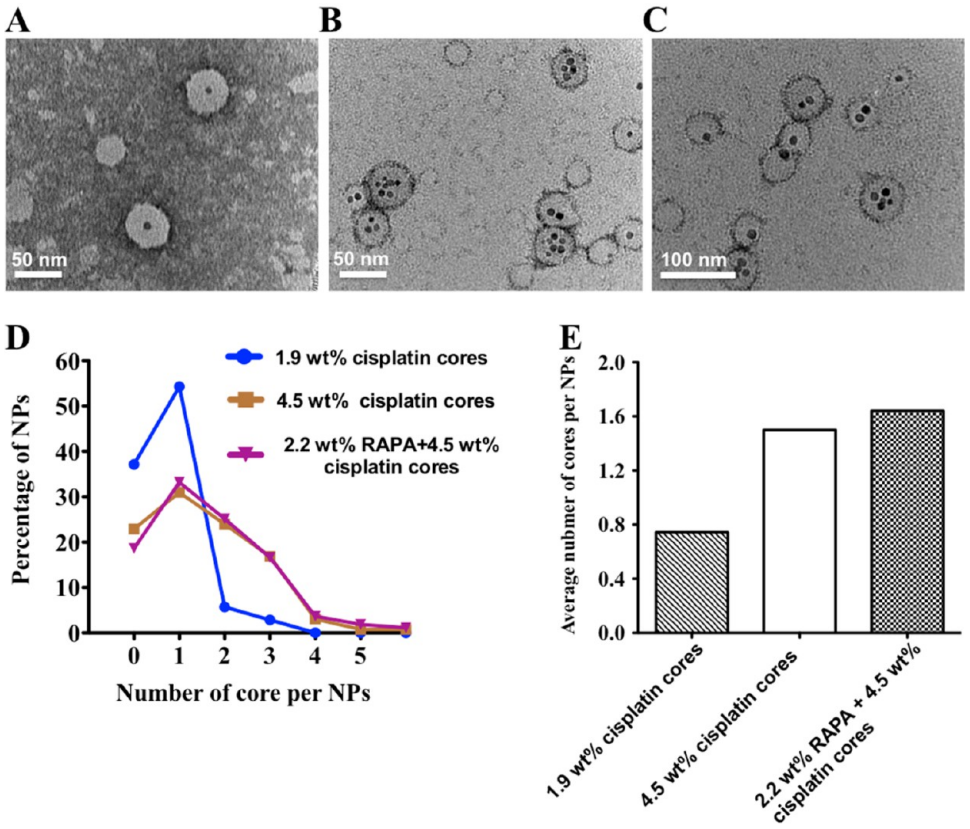

Figure 2. TEM images of PLGA NPs loaded with 1.9 wt % of cisplatin cores (A), 4.5 wt % of cisplatin cores (B), and 2.2 wt % of RAPA and 4.5 wt % of cisplatin cores (C). All NPs were negatively stained with uranyl acetate. The number of cisplatin cores per PLGA NP (D and E) can be controlled by altering its feed ratio and is not affected by the presence of RAPA. More than 100 NPs were analyzed.

Analysis of the physical characteristics of all PLGA NPs was performed by transmission electron microscopy (TEM). PLGA NPs were spherical with a diameter of approximately 50 nm (Figure 2, A−C), smaller than the value determined by dynamic light scattering (DLS) (Figure 1 and Figure S1, Supporting Information). TEM analysis also revealed that increases in the feed ratio of cisplatin cores resulted in subsequent increases in the average number of cisplatin cores per PLGA NP (Figure 2, A and B). However, the morphology and loading of cisplatin cores was unaffected by the presence of RAPA (Figure 2, B and C). We have analyzed over 100 PLGA NPs to determine the distribution profile regarding the average number of cisplatin cores. The distribution profiles for three different formulations were determined with two different concentrations of cisplatin cores and one (RAPA + cisplatin cores) combination. Figure 2D indicates that the vast majority of PLGA NPs contained one to three cisplatin cores. Therefore, most of our NPs are able to utilize the synergy between cisplatin and RAPA. We calculated the average number of cisplatin cores as 0.74, 1.5, and 1.6 for PLGA NPs with 1.9 wt % cisplatin cores, 4.5 wt % cisplatin cores, and (2.2 wt % RAPA + 4.5 wt % cisplatin cores) ratios, respectively (Figure 2E). These results indicate that the incorporation of RAPA into PLGA NPs did not affect the loading of cisplatin cores. The distribution profile for (2.2 wt % RAPA + 4.5 wt % cisplatin cores) combinatory PLGA NPs (Figure 2, D and E) indicates that only ~20% of PLGA NPs did not contain cisplatin NPs. Because empty RAPA PLGA NPs can only achieve a low loading of RAPA (Figure 1. C), we can conclude that the vast majority of RAPA was coencapsulated alongside cisplatin cores and only a small amount of RAPA was encapsulated alone in PLGA NPs.

Therefore, this is the first time that hydrophobic cisplatin cores and RAPA were coencapsulated into a single PLGA NP with a high drug loading through a solvent displacement method. Furthermore, cisplatin cores were found to further enhance the loading of RAPA into PLGA NPs. Because of the flexibility of this platform, further investigations into the interaction between hydrophobic, inorganic NPs, and hydrophobic drugs may lead to the development of new, efficient drug loading mechanisms tuned for facilitating the codelivery of drugs working at synergistic ratios. Co-encapsulation of multiple agents with diverse physicochemical properties, such as calcium phosphate cores loaded with gemcitabine and macromolecular siRNA, may be possible.[22,24]

Cellular Uptake of PLGA NPs in A375-luc Melanoma Cells. The use of anisamide to bind overexpressed sigma

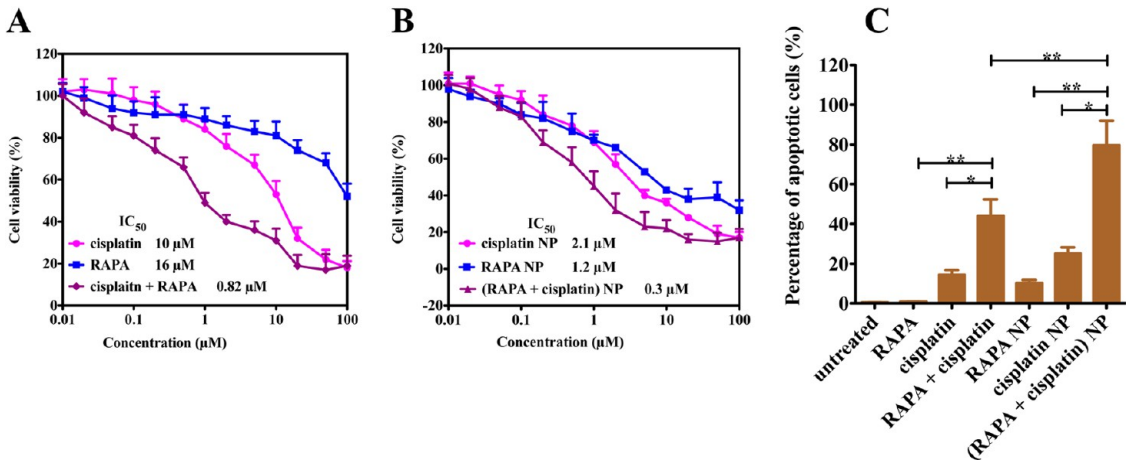

Figure 3. Cell toxicity of free RAPA, cisplatin, and their combination in A375-luc cells (A); cell toxicity of RAPA PLGA NPs, cisplatin PLGA NPs, and combinatory PLGA NPs in A375-luc cells (B). IC_{50} of free drug combination and combinatory PLGA NPs were calculated based on the concentration of cisplatin. Cells were stained with Annexin V-FITC/PI, and the number of apoptotic cells was counted by flow cytometry. Apoptosis of A375-luc cells induced by incubation with drugs for 24 h (C). The loading of cisplatin cores and RAPA in combinatory PLGA NPs was 4.5 and 2.2 wt %, respectively; the loading of cisplatin in cisplatin PLGA NPs was 4.5 wt %; the loading of RAPA in RAPA PLGA NPs was 0.8 wt %. * indicates $P < 0.05$; ** indicates $P < 0.01$.

receptors on human tumors is a well-known and accepted method for achieving preferential NP accumulation in tumors. Sigma receptors are well-known membrane-bound proteins that show high affinity for neuroleptics and are overexpressed on many human tumors including melanoma, non-small cell lung carcinoma, breast tumors of neural origin, and prostate cancer.[31−33] Sigma receptors bind to haloperidol and various other neuroleptics showing a high affinity with the anisamide moiety. We therefore synthesized PLGA-PEG-MBA (as described in Figure S2, Supporting Information) for the enhanced delivery of RAPA and cisplatin cores into A375-luc melanoma tumor cells.

In vitro cellular uptake of PLGA-PEG-MBA NPs was measured using ICP-MS. Compared to the free drugs alone, PLGA-PEG-MBA NPs loaded with only cisplatin cores, or cisplatin cores alongside RAPA, facilitated greater cellular uptake of cisplatin in A375-luc cells than the treatments not utilizing anisamide (Figure S3, Supporting Information). Quantitative ICP-MS results clearly indicated that the MBA ligand furthered NP uptake by approximately 2-fold. Receptor competition experiments further showed that haloperidol could effectively compete with MBA in binding to sigma receptors on A375-luc cells, suggesting MBA modification induced sigma receptor-mediated endocytosis (Figure S3, Supporting Information). Because of the advantages of employing anisamide mediated cell uptake, all PLGA NPs were composed of PLGA-PEG-MBA containing the specified drug or drugs unless otherwise stated.

Cell Toxicity and *in Vitro* Synergistic Effects. It has been reported that RAPA is capable of sensitizing melanoma cells to cisplatin.[19−21] PLGA NPs loaded with a 4.5 wt % of cisplatin cores and 2.2 wt % of RAPA corresponding to a cisplatin/RAPA molar ratio of 5.5:1 were formulated to employ this synergy. First, we evaluated the degree of synergy between free RAPA and cisplatin by characterizing their cytotoxicity toward A375-luc cells *in vitro* separately and in combination. The IC_{50} of free cisplatin and RAPA administered separately was 10 and 16 μM, respectively. However, a combination of free cisplatin and RAPA resulted in a much lower IC_{50} of 0.82 μM (based on the concentration of cisplatin) (Figure 3, A). A combination index (CI) was determined using the Chou−Talalay isobologram equation.[13,14] The CI at the IC_{50} of the free drug combination was 0.36, indicating strong synergism. For the NPs, the IC_{50} of cisplatin PLGA NPs and RAPA PLGA NPs were 2.1 and 1.2 μM, respectively, which demonstrated 5- and 13-fold decreases over free cisplatin and RAPA, respectively (Figure 3, B). Yet, coencapsulation of both drugs into single PLGA NP permits an even lower IC_{50}. In the combinatory PLGA NPs, the IC_{50} achieved through coencapsulation was approximately 0.3 μM (based on the concentration of cisplatin). The CI at the IC_{50} was 0.5, which also indicated synergism. In addition, empty PLGA NPs did not induce any cytotoxicity (Figure S4, Supporting Information).

After treatment, A375-luc cell apoptosis was assayed using FITC-Annexin V/PI staining. The number of apoptotic cells was then quantified using flow cytometry (Figure 3, C). Results indicated that RAPA significantly sensitized A375-luc melanoma cells to apoptosis induced by cisplatin, possibly because mTOR inhibitors sensitize tumor cells to cisplatin by blocking the up-regulation of p21 and inducing apoptosis as a result.[19−21]

Because the presence of cisplatin cores greatly enhanced the loading of RAPA into PLGA NPs, the efficacy of a formulation composed of two separate NPs, RAPA PLGA NPs, and cisplatin PLGA NPs

administered as separate nanoparticles was not determined. It is believed that the loading of RAPA in this case would be insufficient to achieve the synergistic ratio with cisplatin. Additionally, the efficacy of the combination therapy relies heavily on maintaining the synergistic ratio between cisplatin and RAPA. With two separate NPs, the ratio may not be effectively maintained *in vivo* because their distributions may vary following administration. Thus, the *in vitro* and *in vivo* anticancer efficacy of RAPA PLGA NPs, cisplatin PLGA NPs, and combinatory PLGA NPs were compared, but anticancer activity of a combination of cisplatin PLGA NPs and RAPA PLGA NPs was not tested.

Sustained Release of RAPA and Cisplatin without Burst Release. To fully utilize the advantages of combination therapy, the *in vitro* release of both drugs at the desired molar ratio for employing synergy is crucial. We measured the release of cisplatin and RAPA from combinatory PLGA NPs using ICP-MS and high-performance liquid chromatography (HPLC) (Figure 4). Combinatory NPs showed sustained release of both cisplatin and RAPA. Moreover, combinatory PLGA NPs exhibited a similar release rate for both cisplatin and RAPA, which will further enhance the synergistic effects as expected. In addition, the release rate of cisplatin from combinatory PLGA NPs was only slightly affected by the presence of RAPA. The release of RAPA from combinatory PLGA NPs followed the same pattern as the release of cisplatin. It is notable that no burst release pattern was observed. *In vitro* release results indicated the burst release of cisplatin from cisplatin PLGA NPs was circumvented by the hydrophobic DOPA coating, which is very difficult to achieve in other PLGA-based cisplatin particles. As a result, the encapsulation of hydrophilic drugs in lipid-coated cores may offer a novel strategy to overcome the prominent burst release issue.

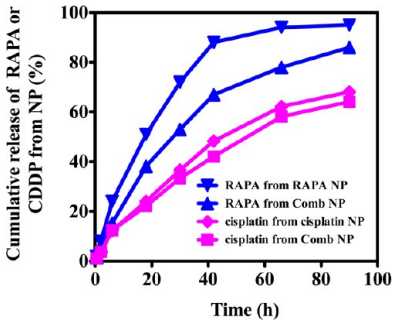

Figure 4. *In vitro* **release kinetics of cisplatin and RAPA in PBS at 37 °C from PLGA NPs. The loading of cisplatin cores and RAPA in combinatory PLGA NPs was 4.5 and 2.2 wt %, respectively; the loading of cisplatin in cisplatin PLGA NPs was 4.5 wt %; the loading of RAPA in RAPA PLGA NPs was 0.8 wt %.**

Pharmacokinetics and Biodistribution. In order to study the pharmacokinetics (PK) and biodistribution of both the drugs and the PLGA carrier, two methods were used. Quantification of RAPA and PLGA was achieved through a ^{14}C and ^{3}H label, respectively, while the concentration of cisplatin was determined through ICP-MS. The PK data were fitted with a non-compartment model using the WinNonlin program. The PK experiment indicated a prolonged blood circulation time for the combinatory PLGA NPs (Figure 5, A). After intravenous injection, about 40% of the combinatory PLGA NPs were still in the blood after 1 h, while the free drug was rapidly cleared within 20 min.[43] The $t_{1/2}$ is about 2.5 h. It was found that there was no significant difference in PK among ^{14}C labeled RAPA (^{14}C-RAPA), cisplatin, and ^{3}H-labeled combinatory PLGA NPs (Figure 5, A), indicating negligible release of drugs from combinatory PLGA NPs during the circulation. Eight hours post-iv injection, 6.0% of the injected dose per gram of cisplatin in combinatory NPs accumulated in the tumor (Figure 5, B), which was significantly higher than free CDDP.[25] Meanwhile, the accumulation ratio of ^{14}C-RAPA/cisplatin/^{3}H-labeled combinatory NPs was near 1:1:1. Therefore, combinatory PLGA NPs delivered cisplatin and RAPA at synergistic ratio into tumor without significant release of drug during the circulation in the blood. It was also found that liver was the major organ to clear PLGA NPs,

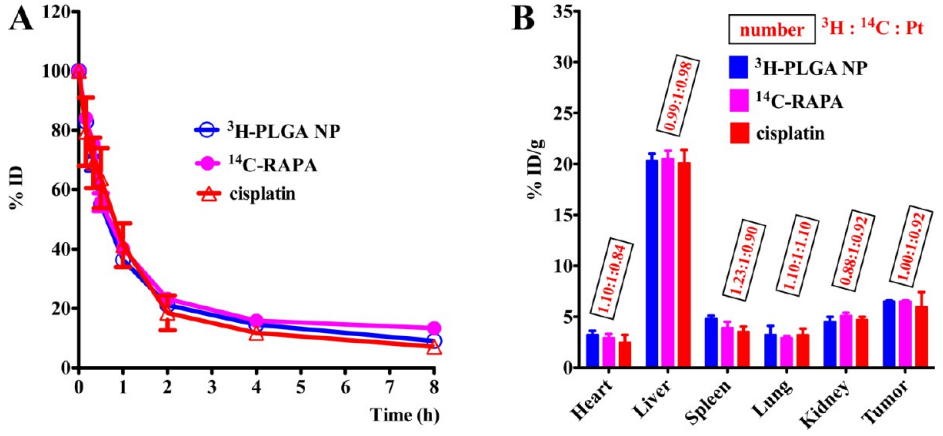

Figure 5. Pharmacokinetics (A) and biodistribution (B) of combinatory NPs in A375-luc tumor-bearing nude mice. PLGA and RAPA were labeled with ^{3}H and ^{14}C, respectively, and were measured using scintillation counter.

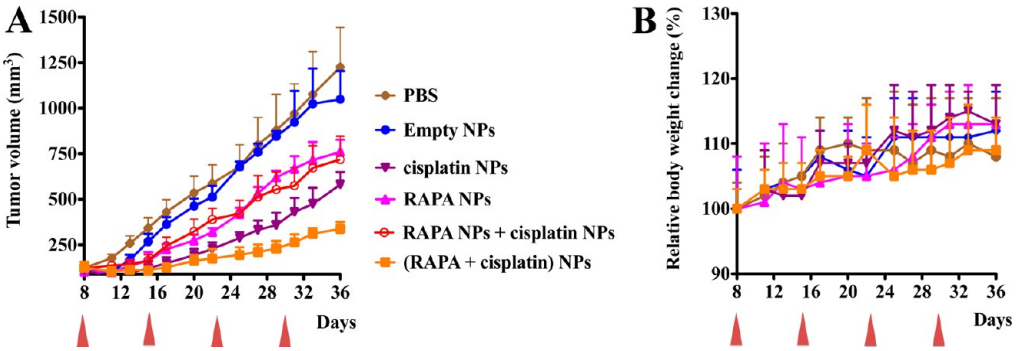

Figure 6. Effects of empty PLGA NPs, RAPA PLGA NPs, cisplatin PLGA NPs, mixture of cisplatin PLGA NPs and RAPA PLGA NPs, and combinatory PLGA NPs on tumor growth (A) and body weight (B) respectively of A375-luc tumor bearing mice. The arrowheads indicate the time of injection. RAPA was administered intravenously at a dose of 0.15 mg/kg; cisplatin was administered intravenously at a dose of 0.3 mg/kg. The loading of cisplatin cores and RAPA in combinatory PLGA NPs was 4.5 and 2.2 wt %, respectively; the loading of cisplatin cores in cisplatin PLGA NPs was 4.5 wt %; the loading of RAPA in RAPA PLGA NPs was 0.8 wt %. The results are displayed as mean ± SEM (error bars) of four animals per group.

which is consistent with the biodistribution of other PLGA NPs.[44]

***In Vivo* Combinatory PLGA NPs Inhibited the Growth of A375-luc Xenograft Tumor Notably and Safely.** As previously mentioned, one of the most fundamental principles behind this formulation is based on the observation that cisplatin cores significantly enhanced the loading of RAPA into PLGA NPs. Therefore, it would be intuitive and convenient to codeliver cisplatin cores and RAPA in a single nanoparticulate formulation at a synergistic ratio *in vivo*.

Mice bearing subcutaneous A375-luc tumors were treated with a dose of 0.15 mg/kg RAPA or 0.3 mg/kg cisplatin on a weekly basis. The combinatory treatment group was given both drugs at the previous ratio on a weekly basis. As shown in Figure 6, combinatory PLGA NPs exhibited significant anticancer activity without reducing the body weight of treated animals. We also showed that combinatory PLGA NPs were more efficacious than a mixture of RAPA PLGA NPs and cisplatin PLGA NPs administered at the same time in different carriers (Figure 6), further verifying the importance of codelivery of synergistic drugs in the same carrier to maintain the synergistic ratio of drugs in the tumor cells both *in vitro* and *in vivo*. H&E staining further confirmed the absence of observable nephrotoxicity (Figure S5, Supporting Information), thus supporting the basis that combinatory PLGA NPs are both efficacious and safe.

Combinatory PLGA NPs Reduced Stroma and Induced Significant Apoptosis of TAFs and Tumor Cells. A dense extracellular matrix (ECM) and the stromal components of tumors contribute to an increased interstitial fluid pressure (IFP), which severely hampers efficient penetration of NPs into the tumor.[45] As a result, cells distal from blood vessels are resistant to systemic therapy because of low drug availability. Hence, targeting non-neoplastic components within the microenvironment provides an alternative opportunity for developing more effective therapy.

Therapeutic evaluations showed that combinatory PLGA NPs exhibited considerable anticancer efficacy even when administered weekly at a low dose (0.3 mg/kg cisplatin; 0.15 mg/kg RAPA). We postulated that the success in tumor growth inhibition may be induced by microenvironment specific effect. By weakening the protective tumor microenvironment, drug-loaded NPs exhibited enhanced penetration into tumor cells and subsequently enhanced efficacy. We therefore examined whether treatments affected the tumor microenvironment. First, collagen, a major extracellular matrix component, was stained using Masson Trichrome assay. As shown in Figure 7, combinatory PLGA NP treatment significantly reduced the amount of collagen (blue) by approximately 80% compared to an untreated control. However, we observed that cisplatin PLGA NPs and RAPA PLGA NPs were unable to reduce as much collagen.

As collagen is secreted by TAFs (tumor-associated fibroblasts), the effect of this treatment on TAFs was further investigated by staining for α-smooth muscle actin (SMA), a marker of TAFs.[46] Apoptosis was confirmed through terminal deoxynucleotidyl transferase dUTP nick end labeling (TUNEL) (Figure 8). As shown in Figure 8, cisplatin PLGA NPs and combinatory PLGA NPs induced significant apoptosis in tumor cells, greatly reduced the fibroblast population, and therefore, potentially decreased the level of collagen. Five randomly selected microscopic fields contained 0.4% TUNEL-positive cells on average in the control group, 7.8% in the RAPA-treated group, 14.2% in the cisplatin-treated group, and 66.2% in the combination therapy group. α-SMA staining results supported that A375-luc xenograft tumors are abundant in TAFs because 25.1% of control group cells were TAFs. Combinatory PLGA NPs almost completely depleted these cells with only 2.2% SMA-positive cells remaining following combinatory treatment. Nevertheless, RAPA PLGA NPs alone did not affect the amount of TAFs. It is notable that MBA-modified combinatory PLGA NPs not only affected

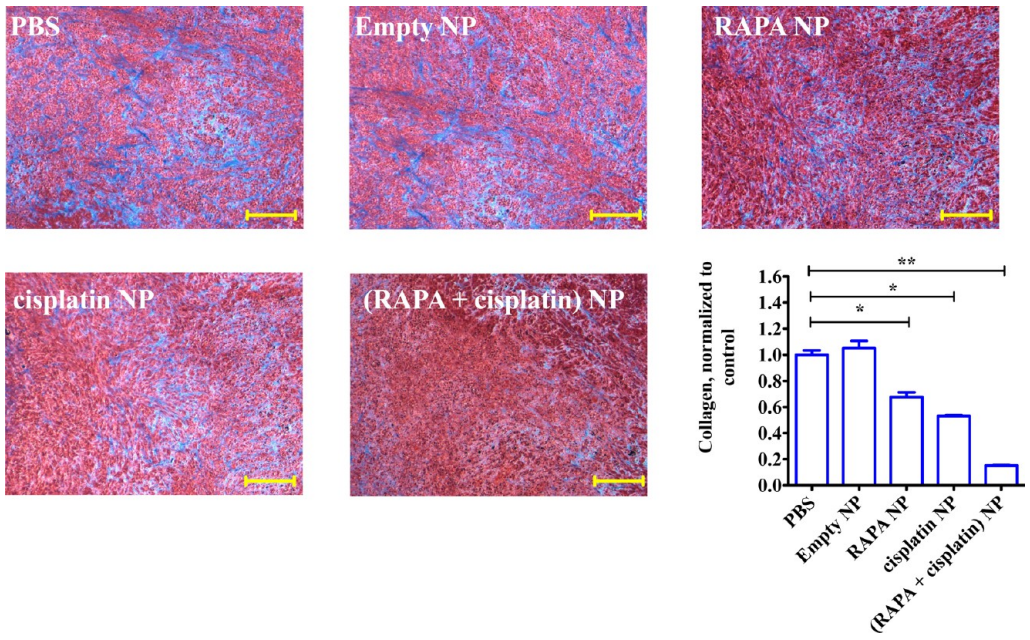

Figure 7. Tumor sections were stained with Masson Trichrome. The blue color represents collagen content, and the cytoplasm is stained red. The collagen content of five randomly selected microscopic fields was quantified using ImageJ. * indicates $P < 0.05$; ** indicates $P < 0.01$. The scale bar represents 100 μm.

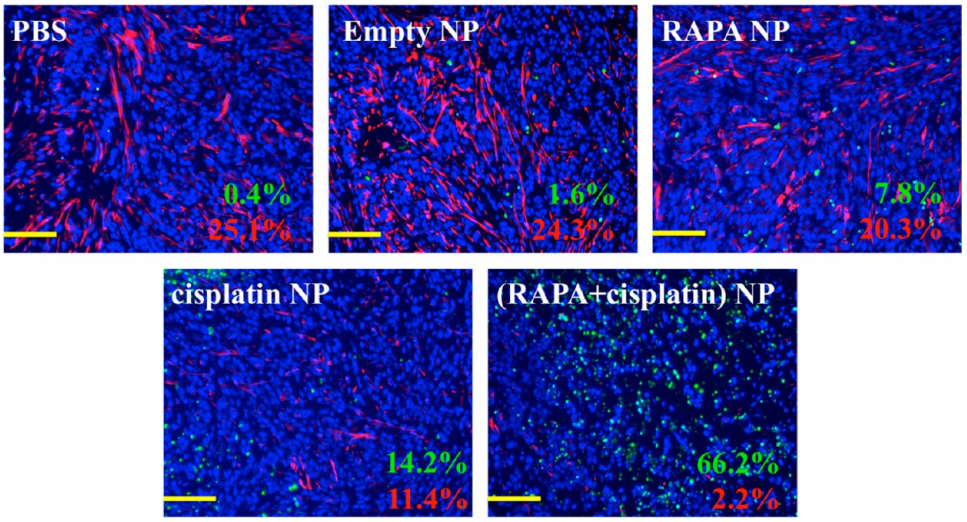

Figure 8. TAFs were stained by α-SMA antibody (red) and apoptosis of cells in A375-luc tumors was indicated by TUNEL assay (green). Nuclei are stained blue. The percentage denotes the average percentage of α-SMA$^+$ fibroblasts (red) and the percentage of TUNEL positive cells (green), respectively. Five randomly selected microscopic fields were quantitatively analyzed on ImageJ. The scale bar represents 100 μm.

tumor cells but also depleted TAFs. This observation indicates that while MBA can enhance the uptake of combinatory PLGA NPs by tumor cells, its delivery is not specific to tumor cells only. Through depletion of TAFs and a reduction of collagen expression, combinatory PLGA NPs may achieve a greater perfusion of NPs into tumor cells for enhanced therapeutic effects. Thus, the presence of RAPA greatly modulated the tumor microenvironment to facilitate enhanced drug penetration and efficacy. However, RAPA alone is still less effective than a combination of cisplatin and RAPA at a synergistic ratio.

Combinatory NPs Showed an Antiangiogenesis Effect and Normalized Tumor Vessels. Angiogenesis is required for invasive tumor growth and metastasis. Therefore, it constitutes an important point in the control of cancer progression and a target to inhibit further growth.[47] Unlike normal blood vessels, the tumor vasculature is abnormally composed, resulting in the formation of physiological barriers which hamper the delivery of therapeutic agents into tumors.[48] Therefore, antiangiogenic imbalances in the tumor results in tumor vasculature normalization and thus improves NP delivery and accumulation in the tumor.[48] Combination of

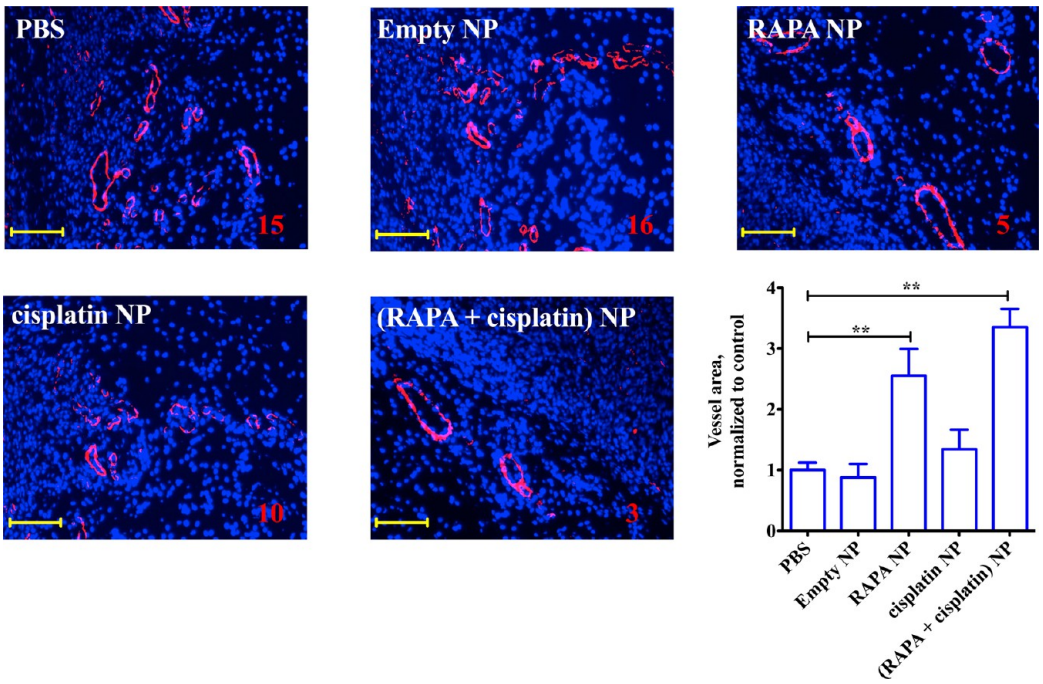

Figure 9. Antiangiogenesis effect of treatments on the A375-luc xenograft tumor was investigated by CD-31 staining (red). Nuclei were stained blue. The number denotes the average number of CD-31 positive vessels per microscopic field. Vessel area, quantified using ImageJ, was normalized to a PBS treated control. Five randomly selected microscopic fields were quantitatively analyzed on ImageJ. * indicates $P < 0.05$; ** indicates $P < 0.01$. The scale bar represents 100 μm.

cytotoxic therapies and antiangiogenic treatment during the vascular normalization also exhibits synergistic effects.

To study the antiangiogenesis effect of the NPs, blood vessels were stained using an anti CD31 antibody (Figure 9). Mice treated with RAPA PLGA NPs alone and combinatory PLGA NPs exhibited a marked decrease in the number of vessels in tumor. However, the number of blood vessels in the tumor in mice treated with cisplatin PLGA NPs alone was only slightly affected by the treatment. In addition, blood vessel normalization was observed with RAPA treatment groups, consistent with previous reports in breast cancers.[17,45,49] Normalization may enhance transvascular flux and improve the delivery of NPs to the tumor. To characterize blood flow, the vessel area was quantified by ImageJ and normalized to data from the control group. RAPA PLGA NPs and combinatory PLGA NPs significantly re-expanded the microvasculature and increased the vessel area by approximately 2.5- and 3-fold over the PBS control group, respectively (Figure 9). However, NP formulations employing only cisplatin without RAPA did not exhibit blood vessel normalization.

Combinatory PLGA NPs Improved NP's Penetration in A375-luc Tumor. An elevated IFP, a physical barrier from the extra cellular matrix, hinders the delivery of drugs into the dense collagen matrix.[45] Our studies have shown that combinatory PLGA NPs modulated the stroma by depleting TAFs and decreasing the amount of collagen. In order to study whether these treatment regimens affect the distribution of NP's in A375-luc tumor, DiI containing PLGA NPs (DiI PLGA NPs) were injected following the therapy experiment and mice were sacrificed 24 h post intravenous administration. The blood vessels of tumor were stained using an anti CD31 antibody (green). As shown in Figure 10, RAPA PLGA NPs and combinatory PLGA NPs re-expanded the abnormal blood vessels and decreased the number of blood vessels compared to the untreated group, which is consistent with data mentioned above. In an IFP elevated, untreated tumor, major DiI PLGA NPs were trapped in blood vessels and were unavailable to tumor cells. Although RAPA PLGA NPs enhanced penetration of DiI PLGA NPs, the enhancement was unimpressive. As expected, cisplatin PLGA NPs and combinatory NPs ablated the physical barrier and significantly improved NP delivery into the tumor.

Mechanism of RAPA for Enhancing the Therapeutic Efficacy of Cisplatin. As observed through both clinical and research data, weakening the tumor stroma has proven successful in enhancing the efficacy of chemotherapy. For example, abraxane was combined with gemcitabine to treat pancreatic cancer in a phase I/II study.[50,51] The combination showed significant anticancer efficacy with a 48% response rate, which was attributed to the depletion of stroma for enhanced penetration of gemcitabine inside the pancreatic tumor. Preclinical data have also shown that PEGylated Cellax reduced the content of α-smooth muscle actin, which is a marker of TAFs, in 4T1 and MDA-MB-231 orthotopic breast tumor models.[5] Cellax treatment significantly

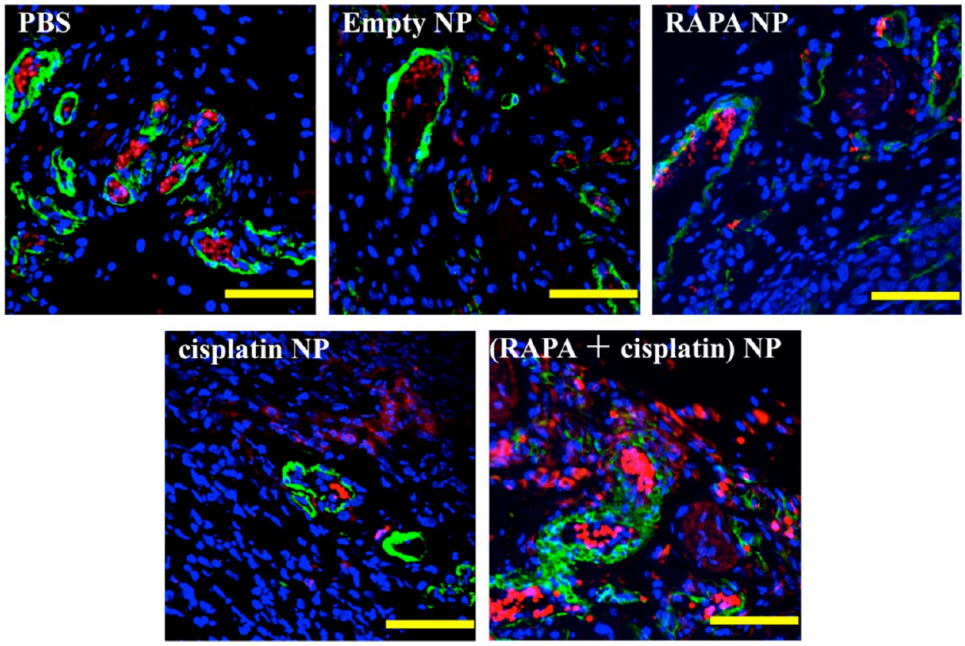

Figure 10. Fluorescent images of the tumor section showed that combinatory NPs improved the penetration of DiI PLGA NP in an A375-luc xenograft. The blood vessels were stained using an anti CD31 antibody (green); the cell nucleus was stained using DAPI (blue); the PLGA NP was labeled with DiI (red). The scale bar represents 50 μm.

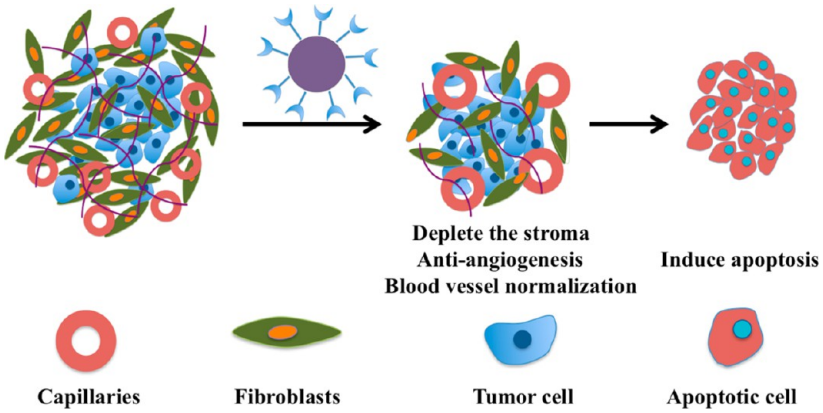

Figure 11. RAPA and cisplatin combination remodeled the tumor microenvironment. Combinatory PLGA NPs exhibited a considerable antiangiogenesis effect and blood vessel normalization and also depleted the stroma.

decreased the IFP of tumor. As a result, the perfusion of active drugs into tumors was significantly enhanced, resulting in a notable tumor growth inhibition. These studies indicated the importance of overcoming stroma-induced barriers in cancer treatment.

In this study, we have successfully engineered combinatory PLGA NPs employing both RAPA and cisplatin at a synergistic ratio. Combinatory PLGA NPs were able to significantly modulate the tumor microenvironment against further tumor proliferation (illustrated in Figure 11) and induce notable anticancer efficacy. mTOR inhibitors, such as RAPA, can suppress tumor proliferation by hindering tumor angiogenesis and blood vessel normalization as studied previously.[52] While RAPA PLGA NPs alone were able to decrease the number of blood vessels through antiangiogenic activity and normalize blood vessels,[52] they were unable to significantly enhance penetration of PLGA NPs into the tumor through microenvironment modulation as illustrated in Figure 10. Thus, compared to cisplatin PLGA NPs and combinatory PLGA NPs, RAPA PLGA NPs exhibited the most minimal tumor inhibition of the three (Figure 6). Similarly, cisplatin PLGA NPs alone showed partial antiangiogenic activities (Figure 9), probably through the inhibition of endothelial cells. Yet, normalization of blood vessels did not occur in tumors from mice treated with cisplatin PLGA NPs alone. Compared to RAPA PLGA NPs, however, cisplatin PLGA NPs did deplete a significant amount of TAFs and down-regulate their collagen expression (Figures 7 and 8). By ablating physical barriers that limited the deep penetration of NPs into the tumor (Figure 10), cisplatin PLGA NPs induced considerable anticancer efficacy (Figure 6). However,

their efficacies were far less significant compared to the combinatory PLGA NPs. Combinatory PLGA NPs not only depleted TAFs and decreased the amount of collagen to foster improved penetration of NPs into the tumor (Figure 10) but also significantly modulated the tumor microenvironment by re-expanding blood vessels and increasing blood flow to promote PLGA NP accumulation in the tumor. Because of the synergy between RAPA and cisplatin, the combinatory PLGA NPs induced significant apoptosis on tumor cells *in vitro* and *in vivo* (Figure 3 and 8). This modulation of the tumor microenvironment therefore permits a substantial enhancement in the efficacies of the following chemotherapy treatments. As a result, combinatory PLGA NPs at a low dose of RAPA and cisplatin on a weekly dosing schedule significantly inhibited the growth of tumor (Figure 6).

The tumor microenvironment is composed of the surrounding blood vessels, immune cells, fibroblasts, pericytes, endothelial cells, signaling molecules, and the extracellular matrix,[53] and many important molecular targets in the microenvironment have been identified.[54] Therefore, the tumor microenvironment has become an important aim for maximizing the effects of chemotherapy through combination therapy. For example, recent studies have shown that the administration of low dose TGF-β inhibitor significantly decreases the IFP in the tumor and therefore enhances the accumulation and penetration of NPs.[55,56] However, the hydrophobicity of the TGF-β inhibitor limits its use and the encapsulation multiple drugs into NPs with diverse physicochemical properties has previously proven difficult. However, our delivery system holds the potential to encapsulate both cisplatin and hydrophobic drugs in a single formulation. Previously, our laboratory has successfully encapsulated drugs such as gemcitabine triphosphate,[22] siRNA, DNA,[23] peptide,[25] and other types of hydrophilic phosphorated drugs into DOPA-coated calcium phosphate cores. Although these drugs are diverse in molecular weight and solubility, they might be easily coencapsulated into PLGA NPs in a similar manner, as they have similar surface properties with cisplatin cores. Drug loaded DOPA-LCP cores may also be able to enhance the encapsulation of hydrophobic drugs. Therefore, this PLGA NP platform can open a window for the study of the synergistic effects between chemotherapy drugs and antistromal drugs and to maximize therapeutic efficacy.

CONCLUSIONS

We have developed PLGA NPs capable of coencapsulating cisplatin cores and RAPA to alter the tumor microenvironment for enhanced drug accumulation and further anticancer efficacy. This is the first method to encapsulate cisplatin directly into PLGA NP with efficient loading and encapsulation using solvent displacement technique. When coencapsulated with RAPA, cisplatin cores improved the loading of RAPA by 3.5-fold. A controlled release profile without burst release was demonstrated for both cisplatin and RAPA in the combinatory PLGA NPs. Therefore, the cytotoxicity of the combined drugs was considerably enhanced by PLGA NP delivery system. When combined, RAPA and cisplatin cores in PLGA NPs reduced the number of TAFs and level of collagen expression within xenograft tumors, demonstrated an antiangiogenesis effect, normalized tumor blood vessels, and improved the penetration of NPs in tumor. We propose that these findings can be extended to the development of new theranostic formulations allowing imaging agents, such as IONPs, QDs and up-conversion NPs, to be combined. Hydrophobic and lipid-coated cores containing drugs, such as siRNA containing lipid-coated calcium phosphate cores, can also be efficiently coloaded to treat a variety of diseases with the advantage of utilizing the synergistic activity between individual drug components.

MATERIALS AND METHODS

Materials. tBOC-PEG$_{3500}$-NH$_2$·HCl and mPEG$_{3000}$-NH$_2$·HCl were ordered from JenKem Technology USA, Inc. (Allen, TX). Acid-terminated PLGA (lactide/glycolide (50:50)) was purchased from DURECT Corporation (Pelham, AL). Cisplatin was purchased from Acros Organics (Fair Lawn, NJ). RAPA was purchased from ChemieTek (Indianapolis, IN). Hexanol, Triton X-100, cyclohexane, *p*-anisic acid, 1-ethyl-3-(3-(dimethylamino)-propyl)carbodiimide (EDC), *N*-hydroxysuccinimide (NHS), and *N, N*-diisopropylethylamine (DIPEA) were obtained from Sigma-Aldrich (St. Louis, MO). DOPA was purchased from Avanti Polar Lipids (Alabaster, AL). ^{3}H-Labeled paclitaxel[*o*-benzamido-^{3}H(N)] and ^{14}C-labeled stearic acid were purchased from Moravek Biochemicals and Radiochemicals (Brea, CA).

Preparation of DOPA-Coated Cisplatin Cores. DOPA-coated cisplatin cores were prepared according to our previous publications,[25,26] dispersed in THF, and stored in a glass vial for further use.

Preparation of PLGA/PLGA-PEG-MBA (1:1 wt/wt) NPs Loaded with Different Cargos. The drugs were loaded into PLGA NPs using the solvent displacement method. Typically, the drugs and 10 mg of polymers were dissolved in 200 μL of THF and added dropwise into 2 mL of water under stirring at room temperature. The resulting NP suspension was allowed to stir uncovered for 6 h at room temperature to remove THF. The NPs were further purified by ultrafiltration (15 min, 3000*g*, Amicon Ultra, Ultracel membrane with 50000 NMWL, Millipore, Billerica, MA). Then, the PLGA-PEG NPs were resuspended, washed with water, and collected likewise. The amount of cisplatin was measured using a Varian 820-MS inductively coupled plasma-mass spectrometer (ICP-MS). The amount of RAPA was measured using high-performance liquid chromatography (HPLC) (Waters Corp., Milford, MA). EE and DL were calculated according to the formulas

$$\mathrm{EE} = \frac{\text{amounts of drug in NPs}}{\text{total amount of drug}} \times 100\%$$

$$\mathrm{DL} = \frac{\text{amount of drug in NPs}}{\text{total weight of NPs}} \times 100\%$$

***In Vitro* Release of Cisplatin and RAPA from PLGA NPs.** RAPA concentration was determined by high-performance liquid

chromatography (HPLC), using CLC-ODS-18 column (5 cm, 4.6 × 150 mm; Waters Corp., Milford, MA) maintained at 25 °C, with an ultraviolet detector at 277 nm. The mixture of 60% acetonitrile and 40% water (v/v) was used as a mobile phase and delivered at a flow rate of 0.5 mL min^{-1}. The injection volume was 20 μL, and the retention time was about 5 min. In addition, Pt concentrations were measured using ICP-MS.

The dialysis technique was employed to study the release of RAPA and cisplatin from different PLGA NPs in phosphate-buffered saline (PBS) (pH 7.4) with 0.25% Tween-80. RAPA-loaded micelles with a final RAPA concentration of 0.85 mg/mL were placed into a dialysis tube with a molecular weight cutoff of 3000 Da and dialyzed against 15 mL of PBS (pH 7.4) with 0.25% Tween-80 in a thermocontrolled shaker with a stirring speed of 200 rpm at 37 °C. Samples of 200 μL were withdrawn at specified times. RAPA concentration was determined by RP-HPLC; Pt concentrations were measured using ICP-MS.

The samples taken for measurement were replaced with fresh media, and the cumulative amount of drug released into the media at each time point was calculated as the percentage of total drug released to the initial amount of the drug. All experiments were performed in duplicate and the data reported as the mean of three individual experiments.

Apoptosis Assays. Quantification of apoptosis by Annexin V/propidium iodide (PI) staining was performed using a BD ApoAlert annexin V-FITC Apoptosis Kit (BD Biosciences, San Jose, CA) according to the manufacturer's instructions. Both floating and attached cells were collected 24 h after drug treatment. The concentration of RAPA was 0.36 μM, and the concentration of cisplatin was 2.0 μM. The molar ratio of cisplatin to RAPA was 5.5. Cells were analyzed on a FACS Calibur flow cytometer using CellQuest Pro software (version 5.1.1; BD Biosciences, San Jose, CA).

***In Vivo* Anticancer Efficacy.** Animals were maintained in the Center for Experimental Animals (an AAALAC accredited experimental animal facility) at the University of North Carolina. All procedures involving experimental animals were performed in accordance with the protocols approved by the University of North Carolina Institutional Animal Care and Use committee and conformed to the Guide for the Care and Use of Laboratory Animals (NIH publication no. 86-23, revised 1985). Female athymic nude mice, 5−6 weeks old and weighing 18−22 g, were supplied by the University of North Carolina animal facility. Five million A375-luc cells were injected subcutaneously into the mice. After 8 days, the mice were randomly divided into six groups (four mice per group). The mice were treated with weekly IV injections of PLGA NPs and saline as a control. A dose of 0.3 mg/kg of Pt and 0.15 mg/kg of RAPA was administered. Thereafter, tumor growth and body weight were monitored. Tumor volume was calculated using the following formula: $TV = (L \times W^2)/2$, with W being smaller than L. Finally, mice were sacrificed using a CO_2 inhalation method. After the therapeutic experiment was done, major organs were collected after treatment and were formalin fixed and processed for routine H&E staining using standard methods. Images were collected using a Nikon light microscope (Nikon).

Masson Trichrome Staining. Paraffin-embedded tumor sections was deparaffinized and rehydrated. The slides were then stained using a Masson Trichrome kit (St. Louis, MO) according to the manufacturer's instructions.

SMA and TUNEL Assay. Paraffin-embedded tumor sections were sequentially stained with Alexa Fluor 647 for α-SMA (alpha smooth muscle Actin, Abcam, Cambridge, MA) immunofluorescence staining, and FITC for TUNEL Assay. For immunofluorescence on α-SMA, the slides were deparaffinized through xylene and a graded alcohol series. After antigen was retrieved in antigen retrieval buffer (Tris-EDTA buffer, pH 9.0), all of the sections were blocked by 1% bovine albumin (Sigma, St. Louis, MO) for 1 h at room temperature before they were incubated with a primary polycolonal rabbit anti-α-SMA antibody (Abcam, Cambridge, MA) at 1:100 dilution overnight at 4 °C. Immunocomplexes were visualized with the corresponding Alexa Fluor 647-labeled goat anti rat secondary antibody at a 1:100 dilution for 1 h at room temperature in the dark. Slides were then rinsed with PBS, prefixed with 4% formaldehyde. Apoptosis *in situ* was then detected by TdT-dependent dUTP-biotin nick end labeling (TUNEL) assay using apoptosis detection kit (Promega, Madison, WI) according to the manufacturer's instructions. Slides were then rinsed with PBS and coverslipped with Vectashield with DAPI (Vector Laboratories, Burlingame, CA). All staining was evaluated and digital images were acquired by Eclipse Ti−U inverted microscope (Nikon Corp., Tokyo, Japan) × 20 magnification. Five randomly selected microscopic fields were quantitatively analyzed on ImageJ (National Institutes of Health).

CD-31 Antibody Staining. In order to observe the vasculature, the sections were incubated with a 1:250 dilution of CD31 primary antibody (Abcam, Cambridge, MA) at 4 °C overnight followed by incubation with FITC-labeled secondary antibody (1:200, Santa Cruz, CA) for 1 h at room temperature. The sections were also stained by DAPI and covered with a coverslip. The sections were observed using a Nikon light microscope (Nikon Corp., Tokyo, Japan). Five randomly selected microscopic fields were quantitatively analyzed on ImageJ (National Institutes of Health).

Study of NPs' Penetration in Tumor. After tumor therapy experiment was complete, mice were administered with DiI encapsulated in PLGA NP at a dose of 0.1 mg/kg DiI and were sacrificed 24 h postintravenous administration. Tumor was embedded in paraffin and sectioned. Paraffin-embedded tumor sections were stained with CD31 primary antibody (Abcam, Cambridge, MA) at 4 °C overnight followed by incubation with FITC-labeled secondary antibody (1:200, Santa Cruz, CA) for 1 h at room temperature. The sections were also stained by DAPI and covered with a coverslip. The sections were observed using a Nikon light microscope (Nikon Corp., Tokyo, Japan).

Statistical Analysis. Quantitative data were expressed as mean ± SEM. The analysis of variance is completed using a one-way ANOVA. $P < 0.05$ was considered statistically significant.

Conflict of Interest: The authors declare no competing financial interest.

Supporting Information Available: Cell lines, experimental syntheses, characterization of NPs, cellular uptake, cell viability, drug combination analysis, and pharmacokinetic and biodistribution studies are described. This material is available free of charge via the Internet at http://pubs.acs.org.

Acknowledgment. This work was supported by NIH Grant Nos. CA151652, CA151455, and CA149363. We thank Steven Glenn Plonk and Andrew Mackenzie Blair for their assistance in manuscript preparation. We also thank Dr. Feng Liu for providing ^{3}H-paclitaxel.

REFERENCES AND NOTES

1. Avgoustakis, K.; Beletsi, A.; Panagi, Z.; Klepetsanis, P.; Karydas, A. G.; Ithakissios, D. S. Plga-Mpeg Nanoparticles of Cisplatin: *In Vitro* Nanoparticle Degradation, *in Vitro* Drug Release and *in Vivo* Drug Residence in Blood Properties. *J. Controlled Release* **2002**, *79*, 123–135.
2. Heldin, C.-H.; Rubin, K.; Pietras, K.; Östman, A. High Interstitial Fluid Pressure—an Obstacle in Cancer Therapy. *Nat. Rev. Cancer* **2004**, *4*, 806–813.
3. Kalluri, R.; Zeisberg, M. Fibroblasts in Cancer. *Nat. Rev. Cancer* **2006**, *6*, 392–401.
4. Garber, K. Stromal Depletion Goes on Trial in Pancreatic Cancer. *J. Natl. Cancer Inst.* **2010**, *102*, 448–450.
5. Murakami, M.; Ernsting, M. J.; Undzys, E.; Holwell, N.; Foltz, W. D.; Li, S. D. Docetaxel Conjugate Nanoparticles That Target Alpha-Smooth Muscle Actin-Expressing Stromal Cells Suppress Breast Cancer Metastasis. *Cancer Res.* **2013**, *73*, 4862–4871.
6. Diop-Frimpong, B.; Chauhan, V. P.; Krane, S.; Boucher, Y.; Jain, R. K. Losartan Inhibits Collagen I Synthesis and Improves the Distribution and Efficacy of Nanotherapeutics in Tumors. *Proc. Natl. Acad. Sci. U.S.A.* **2011**, *108*, 2909–2914.
7. Loeffler, M.; Kruger, J. A.; Niethammer, A. G.; Reisfeld, R. A. Targeting Tumor-Associated Fibroblasts Improves Cancer

Chemotherapy by Increasing Intratumoral Drug Uptake. *J. Clin. Invest.* **2006**, *116*, 1955–1962.
8. Kano, M. R.; Bae, Y.; Iwata, C.; Morishita, Y.; Yashiro, M.; Oka, M.; Fujii, T.; Komuro, A.; Kiyono, K.; Kaminishi, M. Improvement of Cancer-Targeting Therapy, Using Nanocarriers for Intractable Solid Tumors by Inhibition of Tgf-B Signaling. *Proc. Natl. Acad. Sci. U.S.A.* **2007**, *104*, 3460–3465.
9. Beatty, G. L.; Chiorean, E. G.; Fishman, M. P.; Saboury, B.; Teitelbaum, U. R.; Sun, W.; Huhn, R. D.; Song, W.; Li, D.; Sharp, L. L. Cd40 Agonists Alter Tumor Stroma and Show Efficacy against Pancreatic Carcinoma in Mice and Humans. *Science* **2011**, *331*, 1612–1616.
10. Smalley, K. S.; Haass, N. K.; Brafford, P. A.; Lioni, M.; Flaherty, K. T.; Herlyn, M. Multiple Signaling Pathways Must Be Targeted to Overcome Drug Resistance in Cell Lines Derived from Melanoma Metastases. *Mol. Cancer Ther.* **2006**, *5*, 1136–1144.
11. Jia, J.; Zhu, F.; Ma, X.; Cao, Z.; Li, Y.; Chen, Y. Z. Mechanisms of Drug Combinations: Interaction and Network Perspectives. *Nat. Rev. Drug Discovery* **2009**, *8*, 111–128.
12. Lasithiotakis, K. G.; Sinnberg, T. W.; Schittek, B.; Flaherty, K. T.; Kulms, D.; Maczey, E.; Garbe, C.; Meier, F. E. Combined Inhibition of Mapk and Mtor Signaling Inhibits Growth, Induces Cell Death, and Abrogates Invasive Growth of Melanoma Cells. *J. Invest. Dermatol.* **2008**, *128*, 2013–2023.
13. Chou, T.-C. Theoretical Basis, Experimental Design, and Computerized Simulation of Synergism and Antagonism in Drug Combination Studies. *Pharmacol. Rev.* **2006**, *58*, 621–681.
14. Chou, T.-C. Drug Combination Studies and Their Synergy Quantification Using the Chou-Talalay Method. *Cancer Res.* **2010**, *70*, 440–446.
15. Schnell, C. R.; Stauffer, F.; Allegrini, P. R.; O'Reilly, T.; McSheehy, P. M.; Dartois, C.; Stumm, M.; Cozens, R.; Littlewood-Evans, A.; Garcia-Echeverria, C.; et al. Effects of the Dual Phosphatidylinositol 3-Kinase/Mammalian Target of Rapamycin Inhibitor Nvp-Bez235 on the Tumor Vasculature: Implications for Clinical Imaging. *Cancer Res.* **2008**, *68*, 6598–6607.
16. Guba, M.; von Breitenbuch, P.; Steinbauer, M.; Koehl, G.; Flegel, S.; Hornung, M.; Bruns, C. J.; Zuelke, C.; Farkas, S.; Anthuber, M.; et al. Rapamycin Inhibits Primary and Metastatic Tumor Growth by Antiangiogenesis: Involvement of Vascular Endothelial Growth Factor. *Nat. Med.* **2002**, *8*, 128–135.
17. Zhang, Q.; Bindokas, V.; Shen, J.; Fan, H.; Hoffman, R. M.; Xing, H. R. Time-Course Imaging of Therapeutic Functional Tumor Vascular Normalization by Antiangiogenic Agents. *Mol. Cancer Ther.* **2011**, *10*, 1173–1184.
18. Haddadi, A.; Elamanchili, P.; Lavasanifar, A.; Das, S.; Shapiro, J.; Samuel, J. Delivery of Rapamycin by Plga Nanoparticles Enhances Its Suppressive Activity on Dendritic Cells. *J. Biomed. Mater. Res., Part A* **2008**, *84*, 885–898.
19. Lin, P. Y.; Fosmire, S. P.; Park, S. H.; Park, J. Y.; Baksh, S.; Modiano, J. F.; Weiss, R. H. Attenuation of Pten Increases P21 Stability and Cytosolic Localization in Kidney Cancer Cells: A Potential Mechanism of Apoptosis Resistance. *Mol. Cancer* **2007**, *6*, 16.
20. Mungamuri, S. K.; Yang, X.; Thor, A. D.; Somasundaram, K. Survival Signaling by Notch1: Mammalian Target of Rapamycin (Mtor)-Dependent Inhibition of P53. *Cancer Res.* **2006**, *66*, 4715–4724.
21. Tanaka, K.; Sasayama, T.; Mizukawa, K.; Kawamura, A.; Kondoh, T.; Hosoda, K.; Fujiwara, T.; Kohmura, E. Specific Mtor Inhibitor Rapamycin Enhances Cytotoxicity Induced by Alkylating Agent 1-(4-Amino-2-Methyl-5-Pyrimidinyl)-Methyl-3-(2-Chloroethyl)-3-Nitrosourea (Acnu) in Human U251 Malignant Glioma Cells. *J. Neurooncol.* **2007**, *84*, 233–244.
22. Zhang, Y.; Kim, W. Y.; Huang, L. Systemic Delivery of Gemcitabine Triphosphate *Via* Lcp Nanoparticles for Nsclc and Pancreatic Cancer Therapy. *Biomaterials* **2013**, *34*, 3447–3458.
23. Li, J.; Yang, Y.; Huang, L. Calcium Phosphate Nanoparticles with an Asymmetric Lipid Bilayer Coating for Sirna Delivery to the Tumor. *J. Controlled Release* **2012**, *158*, 108–114.
24. Xu, Z.; Ramishetti, S.; Tseng, Y. C.; Guo, S.; Wang, Y.; Huang, L. Multifunctional Nanoparticles Co-Delivering Trp2 Peptide and Cpg Adjuvant Induce Potent Cytotoxic T-Lymphocyte Response against Melanoma and Its Lung Metastasis. *J. Controlled Release* **2013**, *172*, 259–265.
25. Guo, S.; Wang, Y.; Miao, L.; Xu, Z.; Lin, C. M.; Zhang, Y.; Huang, L. Lipid-Coated Cisplatin Nanoparticles Induce Neighboring Effect and Exhibit Enhanced Anticancer Efficacy. *ACS Nano* **2013**, *7*, 9896–9904.
26. Guo, S.; Miao, L.; Wang, Y.; Huang, L. Unmodified Drug Used as a Material to Construct Nanoparticles: Delivery of Cisplatin for Enhanced Anti-Cancer Therapy. *J. Controlled Release* **2014**, *174*, 137–142.
27. Nasongkla, N.; Shuai, X.; Ai, H.; Weinberg, B. D.; Pink, J.; Boothman, D. A.; Gao, J. Crgd-Functionalized Polymer Micelles for Targeted Doxorubicin Delivery. *Angew. Chem.* **2004**, *116*, 6483–6487.
28. Kim, J.; Lee, J. E.; Lee, S. H.; Yu, J. H.; Lee, J. H.; Park, T. G.; Hyeon, T. Designed Fabrication of a Multifunctional Polymer Nanomedical Platform for Simultaneous Cancer-Targeted Imaging and Magnetically Guided Drug Delivery. *Adv. Mater.* **2008**, *20*, 478–483.
29. Chang, J.-Y.; Yang, C.-H.; Huang, K.-S. Microfluidic Assisted Preparation of Cdse/Zns Nanocrystals Encapsulated into Poly (Dl-Lactide-Co-Glycolide) Microcapsules. *Nanotechnology* **2007**, *18*, 305305.
30. Nehilla, B. J.; Allen, P. G.; Desai, T. A. Surfactant-Free, Drug-Quantum-Dot Coloaded Poly(Lactide-Co-Glycolide) Nanoparticles: Towards Multifunctional Nanoparticles. *ACS Nano* **2008**, *2*, 538–544.
31. Vivero-Escoto, J. L.; Taylor-Pashow, K. M.; Huxford, R. C.; Della Rocca, J.; Okoruwa, C.; An, H.; Lin, W.; Lin, W. Multifunctional Mesoporous Silica Nanospheres with Cleavable Gd (Iii) Chelates as Mri Contrast Agents: Synthesis, Characterization, Target-Specificity, and Renal Clearance. *Small* **2011**, *7*, 3519–3528.
32. Nakagawa, O.; Ming, X.; Huang, L.; Juliano, R. L. Targeted Intracellular Delivery of Antisense Oligonucleotides *via* Conjugation with Small-Molecule Ligands. *J. Am. Chem. Soc.* **2010**, *132*, 8848–8849.
33. Banerjee, R.; Tyagi, P.; Li, S.; Huang, L. Anisamide-Targeted Stealth Liposomes: A Potent Carrier for Targeting Doxorubicin to Human Prostate Cancer Cells. *Int. J. Cancer* **2004**, *112*, 693–700.
34. Gaedeke, J.; Fels, L. M.; Bokemeyer, C.; Mengs, U.; Stolte, H.; Lentzen, H. Cisplatin Nephrotoxicity and Protection by Silibinin. *Nephrol. Dial. Transpl.* **1996**, *11*, 55–62.
35. Spitz, D. R.; Phillips, J. W.; Adams, D. T.; Sherman, C. M.; Deen, D. F.; Li, G. C. Cellular Resistance to Oxidative Stress Is Accompanied by Resistance to Cisplatin: The Significance of Increased Catalase Activity and Total Glutathione in Hydrogen Peroxide-Resistant Fibroblasts. *J. Cell. Physiol.* **1993**, *156*, 72–79.
36. Gregg, R. W.; Molepo, J. M.; Monpetit, V. J.; Mikael, N. Z.; Redmond, D.; Gadia, M.; Stewart, D. J. Cisplatin Neurotoxicity: The Relationship between Dosage, Time, and Platinum Concentration in Neurologic Tissues, and Morphologic Evidence of Toxicity. *J. Clin. Oncol.* **1992**, *10*, 795–803.
37. Marsac, P. J.; Shamblin, S. L.; Taylor, L. S. Theoretical and Practical Approaches for Prediction of Drug−Polymer Miscibility and Solubility. *Pharm. Res.* **2006**, *23*, 2417–2426.
38. Kim, S.; Shi, Y.; Kim, J. Y.; Park, K.; Cheng, J.-X. Overcoming the Barriers in Micellar Drug Delivery: Loading Efficiency, *in Vivo* Stability, and Micelle-Cell Interaction. *Expert Opin. Drug Delivery* **2010**, *7*, 49–62.
39. Lu, Y.; Park, K. Polymeric Micelles and Alternative Nanonized Delivery Vehicles for Poorly Soluble Drugs. *Int. J. Pharm.* **2013**, *453*, 198–214.
40. Ling, Y.; Wei, K.; Luo, Y.; Gao, X.; Zhong, S. Dual Docetaxel/Superparamagnetic Iron Oxide Loaded Nanoparticles for Both Targeting Magnetic Resonance Imaging and Cancer Therapy. *Biomaterials* **2011**, *32*, 7139–7150.
41. Dilnawaz, F.; Singh, A.; Mohanty, C.; Sahoo, S. K. Dual Drug Loaded Superparamagnetic Iron Oxide Nanoparticles for

Targeted Cancer Therapy. *Biomaterials* **2010**, *31*, 3694–3706.
42. Oliveira, R. R.; Ferreira, F. S.; Cintra, E. R.; Branquinho, L. C.; Bakuzis, A. F.; Lima, E. M. Magnetic Nanoparticles and Rapamycin Encapsulated into Polymeric Nanocarriers. *J. Biomed. Nanotechnol.* **2012**, *8*, 193–201.
43. Zhang, J.; Miao, L.; Guo, S.; Zhang, Y.; Zhang, L.; Satterlee, A.; Kim, W. Y.; Huang, L. Synergistic Anti-Tumor Effects of Combined Gemcitabine and Cisplatin Nanoparticles in a Stroma-Rich Bladder Carcinoma Model. *J. Controlled Release* **2014**, *182*, 90–96.
44. Guo, J.; Gao, X.; Su, L.; Xia, H.; Gu, G.; Pang, Z.; Jiang, X.; Yao, L.; Chen, J.; Chen, H. Aptamer-Functionalized Peg-Plga Nanoparticles for Enhanced Anti-Glioma Drug Delivery. *Biomaterials* **2011**, *32*, 8010–8020.
45. Provenzano, P. P.; Cuevas, C.; Chang, A. E.; Goel, V. K.; Von Hoff, D. D.; Hingorani, S. R. Enzymatic Targeting of the Stroma Ablates Physical Barriers to Treatment of Pancreatic Ductal Adenocarcinoma. *Cancer Cell* **2012**, *21*, 418–429.
46. Erez, N.; Truitt, M.; Olson, P.; Arron, S. T.; Hanahan, D. Cancer-Associated Fibroblasts Are Activated in Incipient Neoplasia to Orchestrate Tumor-Promoting Inflammation in an Nf-Kappab-Dependent Manner. *Cancer Cell* **2010**, *17*, 135–147.
47. Carmeliet, P.; Jain, R. K. Angiogenesis in Cancer and Other Diseases. *Nature* **2000**, *407*, 249–257.
48. Jain, R. K. Normalization of Tumor Vasculature: An Emerging Concept in Antiangiogenic Therapy. *Science* **2005**, *307*, 58–62.
49. Fokas, E.; Im, J. H.; Hill, S.; Yameen, S.; Stratford, M.; Beech, J.; Hackl, W.; Maira, S. M.; Bernhard, E. J.; McKenna, W. G.; et al. Dual Inhibition of the Pi3k/Mtor Pathway Increases Tumor Radiosensitivity by Normalizing Tumor Vasculature. *Cancer Res.* **2012**, *72*, 239–248.
50. Neuzillet, C.; Tijeras-Raballand, A.; Cros, J.; Faivre, S.; Hammel, P.; Raymond, E. Stromal Expression of Sparc in Pancreatic Adenocarcinoma. *Cancer Metastasis Rev.* **2013**, 10.1007/s10555-10013-19439-10553.
51. Von Hoff, D. D.; Ramanathan, R. K.; Borad, M. J.; Laheru, D. A.; Smith, L. S.; Wood, T. E.; Korn, R. L.; Desai, N.; Trieu, V.; Iglesias, J. L.; et al. Gemcitabine Plus Nab-Paclitaxel Is an Active Regimen in Patients with Advanced Pancreatic Cancer: A Phase I/Ii Trial. *J. Clin. Oncol.* **2011**, *29*, 4548–4554.
52. Dormond-Meuwly, A.; Dufour, M.; Demartines, N.; Dormond, O. Mtor Inhibition and the Tumor Vasculature. *Curr. Angiog.* **2012**, *1*, 11–19.
53. Hanahan, D.; Weinberg, R. A. Hallmarks of Cancer: The Next Generation. *Cell* **2011**, *144*, 646–674.
54. Hainaut, P.; Plymoth, A. Targeting the Hallmarks of Cancer: Towards a Rational Approach to Next-Generation Cancer Therapy. *Curr. Opin. Oncol.* **2013**, *25*, 50–51.
55. Kano, M. R.; Bae, Y.; Iwata, C.; Morishita, Y.; Yashiro, M.; Oka, M.; Fujii, T.; Komuro, A.; Kiyono, K.; Kaminishi, M.; et al. Improvement of Cancer-Targeting Therapy, Using Nanocarriers for Intractable Solid Tumors by Inhibition of Tgf-Beta Signaling. *Proc. Natl. Acad. Sci. U.S.A.* **2007**, *104*, 3460–3465.
56. Meng, H.; Zhao, Y.; Dong, J.; Xue, M.; Lin, Y. S.; Ji, Z.; Mai, W. X.; Zhang, H.; Chang, C. H.; Brinker, C. J.; et al. Two-Wave Nanotherapy to Target the Stroma and Optimize Gemcitabine Delivery to a Human Pancreatic Cancer Model in Mice. *ACS Nano* **2013**, *7*, 10048–10065.